11-1-2018

Interactome mapping uncovers a general role for numb in protein kinase regulation

Ran Wei
Schulich School of Medicine & Dentistry

Tomonori Kaneko
Schulich School of Medicine & Dentistry

Xuguang Liu
Schulich School of Medicine & Dentistry

Huadong Liu
Schulich School of Medicine & Dentistry

Lei Li
Schulich School of Medicine & Dentistry

See next page for additional authors

Interactome Mapping Uncovers a General Role for Numb in Protein Kinase Regulation*[S]

Ran Wei‡, Tomonori Kaneko‡, Xuguang Liu‡, Huadong Liu‡§, Lei Li‡¶‖, Courtney Voss‡, Eric Liu‡, Ningning He¶‖, and Shawn S.-C. Li‡**‡‡

Cellular functions are frequently regulated by protein-protein interactions involving the binding of a modular domain in one protein to a specific peptide sequence in another. This mechanism may be explored to identify binding partners for proteins harboring a peptide-recognition domain. Here we report a proteomic strategy combining peptide and protein microarray screening with biochemical and cellular assays to identify modular domain-mediated protein-protein interactions in a systematic manner. We applied this strategy to Numb, a multifunctional protein containing a phosphotyrosine-binding (PTB) domain. Through the screening of a protein microarray, we identified >100 protein kinases, including both Tyr and Ser/Thr kinases, that could potentially interact with the Numb PTB domain, suggesting a general role for Numb in regulating kinase function. The putative interactions between Numb and several tyrosine kinases were subsequently validated by GST pull-down and/or co-immunoprecipitation assays. Furthermore, using the Oriented Peptide Array Library approach, we defined the specificity of the Numb PTB domain which, in turn, allowed us to predict binding partners for Numb at the genome level. The combination of the protein microarray screening with computer-aided prediction produced the most expansive interactome for Numb to date, implicating Numb in regulating phosphorylation signaling through protein kinases and phosphatases. Not only does the data generated from this study provide an important resource for hypothesis-driven research to further define the function of Numb, the proteomic strategy described herein may be employed to uncover the interactome for other peptide-recognition domains whose consensus motifs are known or can be determined. ***Molecular & Cellular Proteomics 17: 10.1074/mcp.RA117.000114, 2216–2228, 2018.***

Protein-protein interactions (PPIs)[1] play a pivotal role in all essential cellular processes, and dysregulation of PPI may lead to diseases such as cancer (1). Identification and characterization of the binding partners for a protein is crucial for the systematic understanding of its function. This study is focused on identifying and characterizing the interactome of Numb, originally identified for its role in asymmetric cell division (2–4). At the molecular level, Numb exhibits a complex array of functions and is involved in a multitude of biological processes including ubiquitination-mediated protein degradation, endocytosis, cell adhesion, cell polarity, cell migration and tumorigenesis (5). This wide range of roles is likely because of the ability of Numb to bind to a variety of different proteins. Accordingly, most Numb functions were uncovered through the identification of novel Numb-binding proteins. For instance, Numb was found to play a role in protein ubiquitination by directly interacting with the E3 ligase Mdm2 (6), Lnx1 (7), Itch (8) or Siah1 (9). Numb has also been identified as an endocytic protein as it interacts with the endocytosis regulators EH, EPS15, EPS15R and AP-2 (10, 11) and localizes to the cytoplasmic membrane (12). During endocytosis, Numb mediates the internalization of a number of membrane-associated proteins, including Notch, Integrins, E-cadherin and TrkB, all of which were identified through their interactions with Numb (13–17). Similarly, the function of Numb in cell polarity and migration was discovered along with the identification of Numb-Par complex (Par3/Par6/aPKC) interaction (14–16).

As an adaptor protein, Numb contains a prototypical protein-protein interaction domain, the phosphotyrosine binding (PTB) domain that is evolutionarily and functionally conserved. Based on the SMART database (18, 19), there exist at least 5208 PTB domains from 4530 proteins across different species. The human genome encodes 46 proteins harboring 51 PTB domains. PTB domain-containing proteins are often adaptors and scaffold proteins, which organize and regulate the signaling networks involved in a wide variety of biological processes (20). PTB domains can be divided into three

From the ‡Department of Biochemistry and the Siebens-Drake Medical Research Institute, Schulich School of Medicine and Dentistry, Western University, London, Ontario N6A 5C1, Canada; §Center for Mitochondrial Biology and Medicine, The Key Laboratory of Biomedical Information Engineering of Ministry of Education, School of Life Science and Technology, Xi'an Jiaotong University, Xi'an 710049, Shanxi, China; ¶School of Basic Medical Sciences, Qingdao University, Qingdao 266021, Shangdong, China; ‖College of Pharmacy, Qingdao University, Qingdao 26601, Shangdong, China; **Department of Oncology and Child Health Research Institute, Western University

Received June 7, 2017, and in revised form, December 4, 2017
Published, MCP Papers in Press, December 7, 2017, DOI 10.1074/mcp.RA117.000114

groups: IRS-1/Dok-like, Shc-like, and Dab-like (20). The IRS-1/Dok-like and Shc-like groups bind to their ligands in a phosphotyrosine-dependent manner. The Dab-like group also recognizes tyrosine residues, but the binding is phosphorylation independent. Numb PTB is one of many PTB domains that belong to the latter group. Even though they are not directly involved in tyrosine phosphorylation mediated signaling transduction, Dab-like PTB containing proteins participate in the regulation of various cellular events such as endocytosis (21, 22), membrane protein processing (23, 24), asymmetric cell division (25) and integrin-mediated cell adhesion (26, 27).

Considering the long and continually growing list of proteins that interact with Numb, it is not surprising that Numb has been implicated in cancer as a tumor suppressor. The role of Numb in cancer is mediated, in part, by it interactions with the Notch receptor and the Mdm2/p53 complex. Numb directly binds to Notch (28) and p53 (29) through its PTB domain but regulates Notch and p53 via different mechanisms. Numb promotes the internalization and subsequent degradation of cell membrane-localized Notch, thus attenuating Notch signaling in cell proliferation (13, 30). In contrast, Numb stabilizes p53 by preventing Mdm2-mediated ubiquitination and degradation of p53 (31). Both the Numb-Notch and Numb-p53 interactions bear great potential for the development of novel anti-cancer targeted therapeutics. It is conceivable that a systematic investigation of the Numb interactome would facilitate the exploration of Numb as a therapeutic target. In this regard, several high-throughput methods have been developed for interactome mapping. These include the affinity purification-mass spectrometry (AP-MS), the yeast two-hybrid (Y2H) (32), and the luminescence-based mammalian interactome mapping (LUMIER) (33) approaches.

We have developed an integrated peptide/protein array strategy to map the interactome of Numb, focusing on its PTB domain. Combining protein microarray screening with domain specificity-based prediction, we identified the most expansive interactome for Numb reported to date. Intriguingly, the Numb interactome is characterized with a large number of protein kinases and phosphatases. Our work has greatly expanded the current knowledge of the Numb interactome and suggests a broad role for Numb in regulating cellular functions mediated by protein phosphorylation.

MATERIALS AND METHODS

Reagents and Antibodies—The SKBR3, Hela and HCC78 cell lines were obtained from American Tissue Culture Collection. The H2228 cell line was a gift from Dr. Pasi A. Janne (Dana-Farber Cancer Institute, Boston, MA). The SH-SY5Y cell line was a gift from Dr. Jane R. Rylett (Western University, London, ON). The SKBR3 and HCC78 cells were cultured in RPMI 1640 medium (Sigma, MO, Cat. No. R8758). The Hela and SH-SY5Y cells were cultured in Dulbecco's Modified Eagle Medium (Sigma) supplemented with 2 mM L-glutamine, 100 IU/ml penicillin and 100 μg/ml Streptomycin. Reagents used included Alexa Fluor 647 streptavidin (Thermo Fisher scientific, MA, Cat. No. S21374), rabbit polyclonal anti-Numb (H-70) (Santa Cruz, Cat. No. sc-25668), rabbit monoclonal anti-ALK (Cell signaling, MA, Cat. No. 3633), mouse monoclonal anti-ErbB2 (Thermo Fisher scientific, Cat. No. MA5-13105), rabbit monoclonal anti-ROS1(Cell signaling, Cat. No. 3287), rabbit monoclonal anti-Ret (Cell signaling, Cat. No. 14556), rabbit polyclonal anti-FGR (N-47) (Santa Cruz, Cat. No. sc-130), rabbit monoclonal anti-Flt3 (Cell signaling, Cat. No. 3462).

GST-Numb-PTB Protein Expression, Purification, and Biotinylation—The BL21 strain of *E. coli* was transformed with the pGEX6P3-dNumb-PTB, pGEX6P3-hNumb-PTB plasmids (29, 34). Positive colonies were cultured in Lysogeny Broth (LB) medium to a density of OD600 0.6~0.8, then the protein expression was induced with 0.5 mM IPTG for 16 h at 18 °C. The bacterial cells were harvested and pellets were resuspended in PBS buffer containing a mixture of protease inhibitors (Roche, Cat. No. 04693116001). Triton X-100 was added to a final concentration of 2%, lysozyme at 1 mg/ml and benzonase at 20 units/ml. The suspension was lysed on ice for 30 min. Lysates were centrifuged at 15,000 $\times$ *g* for 30 min at 4 °C and the supernatant was collected. Purification of GST-fused proteins was performed with glutathione Sepharose resin (GE Healthcare Life Sciences, MA, Cat. No. 17075601). The Sepharose was first washed with 10 bed volumes of PBS buffer. The lysate supernatant was then loaded to the resin followed by three column volume washes with PBS buffer, then eluted with 10 mM glutathione in Tris buffer (50 mM Tris-HCl, pH 8.0, 100 mM NaCl) (no elution step for pulldown assays). To determine GST-protein purity, a small amount of the purified protein (or protein on resin) was boiled in SDS-sample buffer and then analyzed by SDS-PAGE followed by Coomassie staining. The GST Numb PTB domains used for the ProtoArray hybridization was biotin-labeled, purified and quantified using the ProtoArray Mini-Biotinylation Kit (Invitrogen, CA, Cat. No. AL-01). The level of protein biotinylation is assessed by comparing the Western blotting signals from streptavidin-HRP between biotinylated GST Numb PTB domains and the biotinylated Gel Standard provided by the Kit.

ProtoArray Hybridization—The ProtoArray (Human protein microarray v4.0, Invitrogen, Cat. No. PAH0524011) was removed from −20 °C and placed immediately at 4 °C for at least 15 min. The array was arranged barcode-side up in each well of a pre-chilled 4-chamber incubation tray. PBST Blocking buffer (1$\times$ PBS, 1% BSA, 0.1% Tween 20) was then added and the buffer immersed microarray slide was incubated for 1 h at 4 °C with gentle rocking. The blocking buffer was then removed and the slide drained. Biotinylated protein probes (120 μl at 50 μg/ml) in probing buffer (1$\times$ PBS, 5 mM $MgCl_2$, 0.5 mM DTT, 0.05% Triton X-100, 5% Glycerol, 1% BSA) was added on top of the microarray surface and a cover glass was carefully placed on the array. The array was blotted for 90 min at 4 °C without shaking. The cover glass was then removed, and the array was washed with the probing buffer 3 times each for 5 min at 4 °C. The array was visualized by incubating with 5 ml Alexa Fluor 647-conjugated streptavidin at a dilution 1:3000 in the probing buffer for 30 min at 4 °C in the dark. Then the array was washed again following the same procedures as above. Finally, the array was dipped into distilled water once to remove salt residues and kept in dark to air dry. The array was scanned on a microarray laser scanner (Tecan Co., Morrisville, NC). Data were analyzed using the Array-Pro analyzer software (Tecan, Co.). Z-score was calculated using the formula: (measured value − average value)/standard deviation. The signals corresponding to the positive and negative control dots were excluded from the Z-score calculation (see also supplemental Table S2 and S3; the Z-scores are under the column "Signal Used").

[1] The abbreviations used are: PPI, protein-protein interactions; SH, Src homology.

Peptide and Peptide Array Synthesis—Both free and membrane-bound peptides (spot arrays) were synthesized on an automatic Intavis AG peptide synthesizer using Fmoc (9-fluorenylmethyl-oxycarbonyl) chemistry. Rink-resin (Rink-NH_2) was used to couple the first amino acid in free peptide synthesis, whereas the amine-derivative cellulose membrane (cellulose-NH_2) was made to couple the first amino acid by on-membrane peptide synthesis. In each synthesis cycle, the carboxyl group of a Fmoc-protected amino acid (Fmoc-AA-COOH) was first linked to the amine group of the previous amino acid (or Rink-NH_2) through an amide bond. All unoccupied amine groups were then blocked (acetylated) by acetic anhydride to prevent incorrect amide bond formation in subsequent cycles. Next, the Fmoc group was removed by piperidine (de-protection) to release the free amine group for coupling to the carboxyl group of the next amino acid residue. Fluorescein-NHS was added at the last coupling cycle to label to the peptide in free peptide synthesis. On completion of synthesis, the peptide spot membrane was treated with a mixture containing 47.5% TFA (trifluoroacetic acid), 1.5% TIPS (tri-isopropylsilane) and 51% H_2O, to remove all remaining side-chain protecting groups. Alternatively, the free peptide-resin was incubated in a mixture containing 95% TFA, 3% TIPS and 2% H_2O to deprotect side chains and cleave the peptide from Rink-resin simultaneously.

Far-Western Blotting of Peptide Array—The peptide spot array membrane was blocked with 3% BSA in TBST buffer (0.1 M Tris-HCl, pH 7.4, 150 mM NaCl, and 0.1% Tween 20) for 1 h at room temperature, with gentle rocking. GST-fusion proteins were added directly into the blocking buffer to reach a final concentration of 1 μg/ml and incubated with the peptide array membrane for 1 h at room temperature, with gentle shaking. The membrane was then washed in TBST buffer three times for 5 min each with shaking. Next, anti-GST-HRP antibody was added at 1:5000 (v/v) into 3% BSA in TBST buffer. The membrane was incubated for 1 h at room temperature with shaking followed by the same washing procedures as above. Finally, the bound GST-protein signal was visualized using ECL and quantified by the Array-Pro analyzer software. The Z-score of a peptide spot was calculated the same way as for a protein dot on the ProtoArray.

Dissociation Constant Determination—The dissociation constant of a PTB-peptide interaction was determined by fluorescence polarization (FP) using fluorescein-labeled peptide (a linker, 6-aminohexanoic acid, was inserted between fluorescein and the first amino acid of the peptide). All binding assays were carried out in Tris Buffer (50 mM Tris-HCl, pH 8.0, 100 mM NaCl, 2 mM DTT) and at least two independent experiments were performed for each peptide. The FP assays were carried out in 384-well flat bottom plates (Corning-3537) and the fluorescence polarization signals detected on an Envision Multilabel Plate Reader (PerkinElmer, Waltham, MA) with excitation set at 480 nM and emission at 535 nm. Binding curves were derived from fitting the isothermal titration data to a hyperbolic nonlinear regression model using Prism 3.0 (GraphPad software, Inc., San Diego, CA). The corresponding dissociation constants (K_d) was also calculated by Prism 3.0.

Immunoprecipitation, GST Pulldown and Western Blotting—Cultured cells were lysed in ice-cold lysis buffer (1% Triton X-100, 50 mM Tris-pH 7.2, 150 mM NaCl, 2 mM $MgCl_2$, 0.1 mM EDTA, 0.1 mM EGTA, 0.5 mM DTT, 10 mM NaF) containing complete protease inhibitors (Roche, Basel, Switzerland). Cell debris was removed by centrifugation, and 500 μg of supernatant protein was incubated for four hours in the presence of 1 μg antibody and 30 μl of 50% slurry protein G Resin (GenScript, NJ, Cat. No. L00209), or 10 μg immobilized GST fusion protein. The beads were subsequently washed three times with lysis buffer and boiled with SDS-loading dye. The precipitates were resolved by SDS-PAGE. Proteins were then transferred to polyvinylidene fluoride PVDF membrane using semi-dry transferring method and detected by immunoblotting with appropriate antibodies and visualized by enhanced chemi-luminescence (ECL).

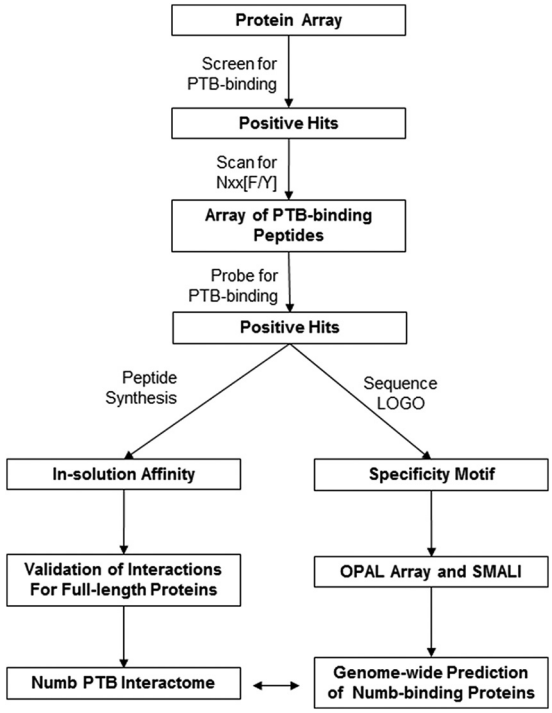

FIG. 1. **Systematic identification of Numb-binding proteins.** A workflow highlighting the strategy used in this study to identify proteins that bind specifically to the Numb PTB domain.

Consensus Binding Motif and Scoring Matrix—OPAL membranes were prepared as previous described (35). Upon binding to the PTB domain, the OPAL membrane was scanned, and the spot intensity quantified on a Bio-Rad imaging system. To generate consensus motifs based on the specific binding signals, the average background signal of the membrane was subtracted from the spot signal. To minimize position-independent effect, the value for each Lys or Arg spot was readjusted by subtracting the average of the Lys or Arg in the column. A scoring matrix was derived from the average, normalized signals for each position of the peptide on two OPAL membranes (36). The scoring matrix was then imported to SMALI and used to search the UniProt protein database (37) to generate a ranked list of potential Numb PTB domain binding peptides/proteins.

RESULTS

Identification of Modular Domain-binding Proteins by Complementary Peptide and Protein Array Screening—We have developed an integrative approach combining protein and peptide array screening with computer-aided ligand prediction to systematically identify the PPI network mediated by modular domains. We evaluated this approach using the Numb PTB domain. As shown in Fig. 1, our workflow started with probing a protein microarray by the purified PTB domain to produce the first interactome. Based on the sequence motif Nxx[F/Y] (where x represents any amino acid residue) recognized by the PTB domain (38, 39), we then scanned this interactome for proteins containing this motif and synthesized the corresponding peptides on a nitrocellulose membrane.

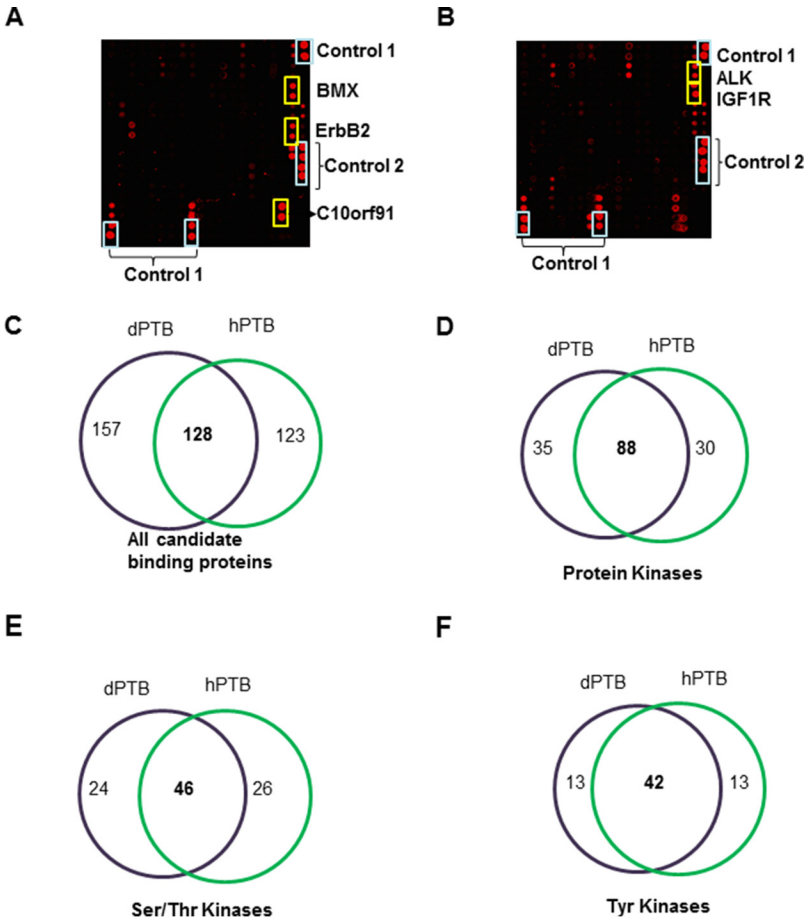

FIG. 2. **A Numb PTB interactome identified by screening a protein microarray.** *A*, *B*, Representative sections of a protein microarray (ProtoArray, Invitrogen) probed with the dNumb PTB domain. Protein spots that showed positive binding (red dots) were labeled. Control 1 spots represent Alexa Fluor 647 Rabbit anti-mouse IgG antibody; Control 2 spots represent Biotinylated anti-mouse antibody. *C*, *A* Venn diagram illustrating all potential binders of the dNumb or hNumb PTB domains identified from screening the ProtoArray and their overlap. *D–F*, Venn diagrams showing the protein kinases that bound the dNumb or/and the hNumb PTB domain.

The resulting peptide spot array was then probed by the Numb PTB, and the positive hits were subsequently validated by in-solution binding assays. Finally, interactions corresponding to high affinity (*i.e.* dissociation constant $K_d < 10$ μM) domain-peptide binding were validated by GST-pulldown or co-immunoprecipitation (IP) using cells expressing the full-length target proteins. In complement to the protein microarray screening, Oriented Peptide Array Library (OPAL) (35) was employed to further define the specificity of the Numb PTB domain and the resulting specificity-profile was used to predict binding proteins at the genome level by the computer program SMALI (36).

Identification of Numb Binding Proteins by Screening a Protein Microarray—To identify binders of the Numb PTB domain in an unbiased manner, we took advantage of a protein microarray (ProtoArray, Invitrogen) that contained 8,274 human proteins (with each protein printed in duplicate; supplemental Fig. S1 and supplemental Table S1). Specifically, the ProtoArray microarray slide was probed with 5 μM of biotinylated, GST-tagged *Drosophila* Numb-PTB (dPTB) or human Numb PTB (hPTB, the isoform lacking the PTB insert (12)) domain. Although the ProtoArray contained only human proteins, we included both the dPTB and hPTB domains in the screen and subsequent binding studies because the two PTB homologues are similar in specificity and the recombinant dPTB protein is more stable than the hPTB (38, 39). The bound proteins were identified by streptavidin labeled with Alexa Fluor 647. The fluorescent signal was recorded on a microarray laser scanner (Fig. 2*A* and 2*B* and supplemental Fig. S2 and 3) and analyzed using the ArrayProxy software (supplemental Figs. S2 and S3, supplemental Table S2 and S3).

Because the duplicate spots of certain proteins on the ProtoArray showed large variations in binding signal (due likely to printing defects), we included in the analysis only proteins for which the average signal over standard deviation is greater than 7.5 or Avg/Std >7.5. A Z-score was then calculated for each protein based on the corresponding Avg value. A protein was considered a positive binder when the $Z \geq 2.0$ (supplemental Figs. S2 and S3). Using these criteria,

we identified 285 candidate binding proteins for dPTB and 251 for hPTB (supplemental Tables S4 and S5) of which 128 were common to both domains (Fig. 2*C*). Intriguingly, 145/408 (>35%) of the identified PTB-binders were protein kinases (Fig. 2*C* and 2*D*). This number increased to >40% when the identified interactome for dPTB and hPTB was analyzed separately (supplemental Figs. S2 and S3). Of the 87 kinases bound to both PTB domains, 46 were Ser/Thr kinase (STK) and 42 are tyrosine kinases (TK) (Fig. 2*E* and 2*F*). Except for PRKCQ, PRKCG, PRKCE, PRKCB, PRKCA and CAMK2B that have been reported as Numb-interacting proteins (40–42), the remaining kinases are new. That the PTB-binding kinases occupy essentially all branches of the human kinome phylogenetic tree (supplemental Fig. S4) suggests that Numb may play a general role in regulating protein kinase function.

Characterization of PTB-binding Motifs in the Numb Interactome Identified from the ProtoArray Screening—The Numb PTB domain is capable of binding to proteins containing the Nxx[Y/F] motif (38, 39). To identify high affinity-binders from the ProtoArray screen, we searched for the presence of this motif in proteins on the ProtoArray that produced a Z-score ≥2.0 when probed with both the dPTB and hPTB domains. This led to the identification of 260 Nxx[Y/F]-containing sequences from 94 proteins. The corresponding peptides were synthesized on a nitrocellulose membrane as a spot array (supplemental Fig. S5*A* and supplemental Table S8). The PTB-binding peptides GLDNPAYVS from human LNX1 and GFSNMSFED from Drosophila NAK (38) were included as positive controls. The LNX1 and NAK peptides containing the N-to-A substitution (39), and the human TrkA peptide (IIENPQYFS) (43) were used as negative controls (supplemental Table S8). The peptide spot array was probed for binding to the purified Numb PTB domain. Because the dNumb PTB domain was more stable than the mammalian counterpart (39), we employed the GST-dPTB protein to probe the peptide array as well as in subsequent binding assays carried out in solution. An anti-GST Far-Western blotting revealed that > 40% peptides on the spot array exhibited binding to the dPTB protein, albeit with large variance in the binding signal (Fig. 3*A*).

Intriguingly, only 19 peptides (excluding the controls) on the spot array yielded signals with a Z-score ≥ 2 (Fig. 3*B*). Because the peptide was 9-aa in length, including 6 residues N-terminal to the [Y/F] that are important for PTB-binding (39, 44), the spot array data suggests that the Nxx[Y/F] motif was insufficient for high-affinity PTB-binding for the majority of peptides examined or that a different region/motif in the corresponding proteins is involved in PTB-binding. To confirm peptide-PTB binding in solution, we synthesized, individually, 12 of the 19 peptides after excluding the 7 peptides that are localized in the extracellular region of the corresponding proteins. The peptides contained a fluorescein tag to facilitate affinity measurement by the fluorescence polarization (FP) assay (38). The dissociation constants of the corresponding dPTB-peptide interactions ranged from 0.5 μM for a peptide derived from ALK to 9.4 μM for an ERBB2-derived peptide (Table I). These values are comparable to those observed for PTB interactions with the control peptides derived from NAK and LNX1, two known Numb PTB-binding proteins (7, 25). It is remarkable that the tyrosine kinase ALK contains three PTB-binding sites, strongly suggesting that Numb and ALK may interact *in vivo*. It should be noted that for peptides that showed strong binding in both the peptide spot array and in-solution binding assay, the corresponding proteins all had Z-scores greater than 3.0 on the ProtoArray (supplemental Tables S2 and S3). Notwithstanding this observation, some proteins with a Z > 3.0, such as C10orf91 and BMX (Fig. 2*A*), do not harbor an Nxx[Y/F] motif, suggesting that these proteins may employ a different mechanism for PTB-binding.

Validation of Selected Numb-kinase Interactions—To validate findings from the ProtoArray screening and peptide binding assays, we carried out GST-pulldown or co-IP experiments to examine the interaction of Numb or Numb-PTB with a selected group of RTKs. The presence of high-affinity binding sequences in ALK, ERBB2 and ROS1 suggest that these kinases may bind to Numb via the PTB domain *in vivo*. Although Numb and ERBB2 were found to co-IP from the breast cancer cell line SK-BR3 (Fig. 4*A*), both the dPTB and hPTB domains were capable of pulling down ALK and ROS1 from cells expressing these proteins in oncogenic fusion forms (Fig. 4*B* and 4*C*). Because not all tyrosine kinases that were positive on the ProtoArray contain the Nxx[Y/F] motif, we tested the binding of a group of RTKs that do not harbor a recognizable motif. As shown in Fig. 4*D*–4*F*, the tyrosine kinases FGR, RET and FLT3 were capable of binding to the Numb PTB domains despite the absence of the Nxx[Y/F] motif, suggesting that additional motifs or modes of binding exist for these proteins. The confirmation of Numb/PTB binding to ALK, ERBB2, ROS1, FGR, RET, and FLT3 in cells, all of which are oncogene products, suggests a role for Numb in cancer pathogenesis via the regulation of oncogenic tyrosine kinases.

Genome-wide Prediction of Numb PTB-binding Proteins—The human genome encodes ~20,000 proteins (45), <50% of which were represented in the protein microarray used in the current study. Some proteins, membrane proteins that are not readily amenable to expression and purification were under represented in the Protoaray. Therefore, to identify Numb-binding proteins at the genome level, we must employ alternative strategies that complement the ProtoArray screening. To this end, we developed a computational approach that allows the prediction of Numb PTB-binding proteins *in silico*. This approach took advantage of the ability of the Numb PTB domain to recognize sequences containing the Nxx[Y/F] motif and the computer program SMALI that was developed previ-

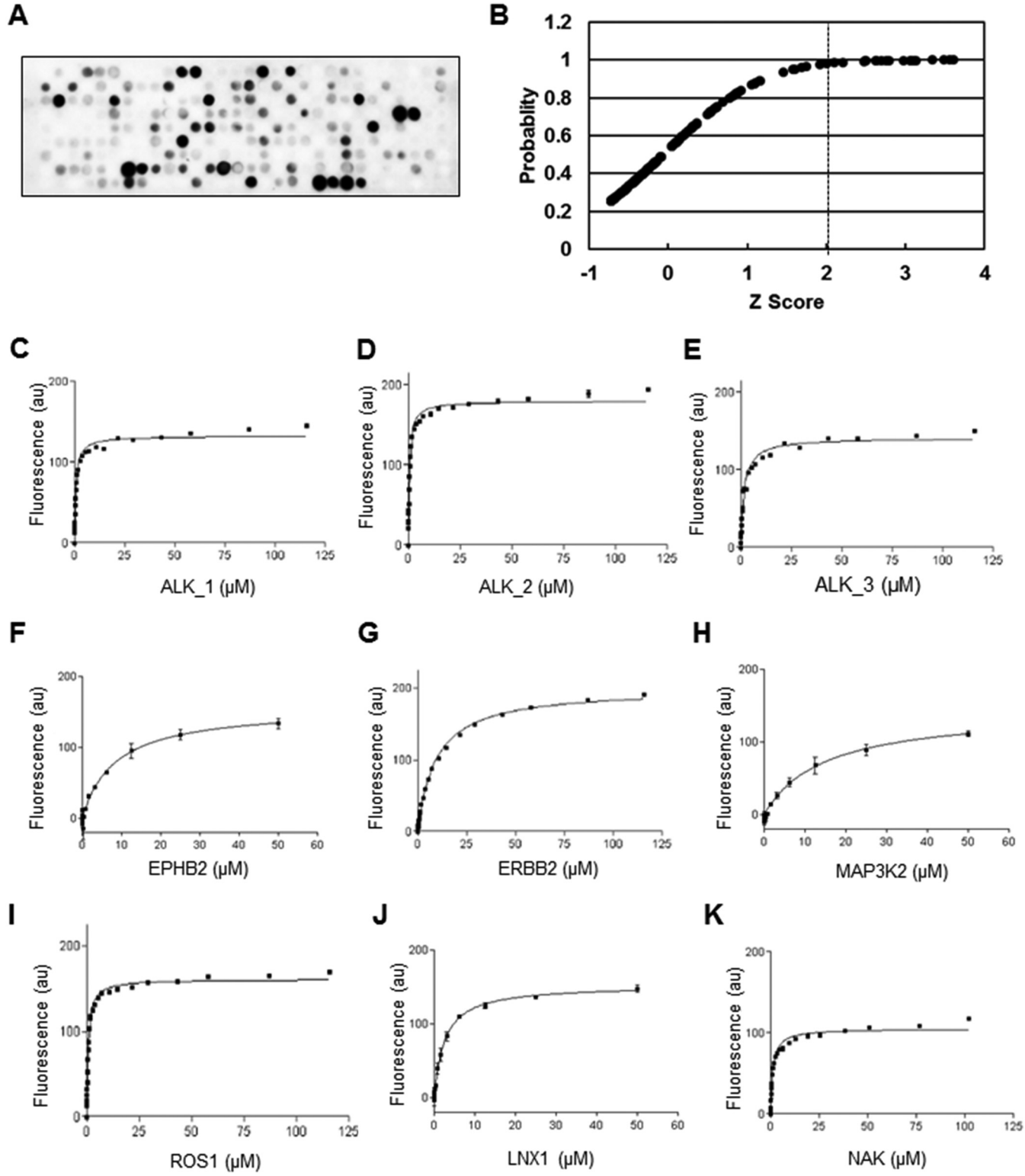

FIG. 3. **Verification of Numb-PTB interactions by peptide array and in-solution binding.** *A*, Binding profile for the dNumb PTB domain on an array of NxxF/Y motif-containing peptides. The peptides were derived from the PTB-interacting proteins identified using the ProtoArray (Fig. 2). *B*, Distribution of Z scores for the positive binders on the peptide array in (*A*). *C–K*, Binding curves of selected peptides from the peptide array for the dNumb PTB domain. See Table I for peptide sequences and K_d values.

TABLE I
Binding affinities of peptides derived from several putative Numb-binding proteins identified in this study

UniProt Entry Name	Gene Name	Peptide Sequence	K_d (μM)	SMALI Score
ProtoArray				
ALK_HUMAN	ALK	CGNVNYGYQQQ	1.6 ± 0.15	1.247
ALK_HUMAN	ALK	GGHVNMAFSQS	0.7 ± 0.04	1.1598
ALK_HUMAN	ALK	FPCGNVNYGYQ	0.5 ± 0.02	0.5257
EPHB2_HUMAN	EPHB2	ESFANAGFTSF	8.3 ± 1.2	1.2428
ERBB2_HUMAN	ERBB2	PAFDNLYYWDQ	9.4 ± 0.3	1.3717
M3K2_HUMAN	MAP3K2	SDYDNPIFEKF	9.1 ± 0.8	1.3775
ROS1_HUMAN	ROS1	SGVINESFEGE	0.7 ± 0.02	1.2859
SMALI prediction				
JIP3_HUMAN	MAPK8IP3	QGIVNKAFGIN	1.5 ± 0.04	1.565
JIP4_HUMAN	SPAG9, MAPK8IP4	KGIENKAFDRN	1.7 ± 0.04	1.5721
PTN13_HUMAN	PTPN13	GGYINASFIKI	2.4 ± 0.49	1.3359
PLSI_HUMAN	PLS1	NPKLNLAFVAN	5.3 ± 0.33	1.497
DUSTY_HUMAN	DSTYK, RIPK5	DIFINQAFDMQ	7.7 ± 0.50	1.7385
SYT1_HUMAN	SYT1	NPYYNESFSFE	8.5 ± 0.35	1.3876
TULP4_HUMAN	TULP4	TDYVNSAFTED	8.5 ± 0.7	1.7111
Control				
LNX1_HUMAN	LNX1	PGLDNPAYVSS	2.5 ± 0.2	1.2611
Q9U485_DROME	NAK	TGFSNMSFEDF	1.1 ± 0.08	1.3358

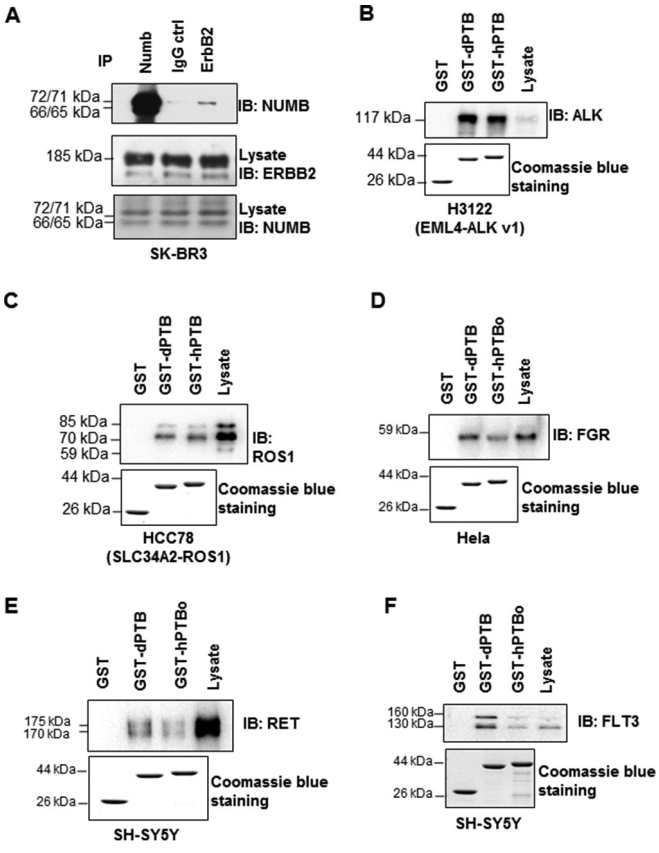

FIG. 4. **Numb or its PTB domain binds to tyrosine kinases in cells.** *A*, ERBB2 co-immunoprecipitated with Numb in SK-BR3 cells. *B–F*, The Numb PTB domains pulled down ALK, ROS1, FGR, RET and FLT3, respectively, from cells expressing these proteins.

ously for the identification of binding ligands for modular interaction domains (36).

Because the Nxx[Y/F] core motif is insufficient to confer high affinity binding (Fig. 2), we further defined the specificity of the Numb PTB domain using the OPAL approach (35). Specifically, we synthesized an OPAL membrane in which the residues N^{-3} and [Y^{O}/F^{O}] were kept constant whereas the other residues were systematically replaced by a naturally occurring amino acid in the degenerated peptide library xxNxxF/Yxx, where x represents a mixture of 19 natural amino acids (except Cys). Probing the OPAL membrane by the dPTB domain yielded a binding pattern that was indicative of its specificity (Fig. 5*A*). Besides showing preference for a hydrophobic residue at the N-terminal region and proclivity for charged amino acids at the C-terminal region to the Nxx[Y/F] core motif, the PTB domain strongly selected for an Ala or Gly at the −1 position within the core motif. Inspection of dPTB in complex with the NAK peptide (GFSNMSFEDFP) (38) reveals that core motif (NMSF) adopts a β-turn structure with the Ser^{-1} residue protruding into a small surface pocket on the PTB domain (supplemental Fig. S6). These characteristics explain why the small residues Ala and Gly are highly preferred for this position. Indeed, replacing the Ser^{-1} residue with Ala led to >850 fold increase in binding affinity for the NAK peptide (39).

Based on the OPAL binding data, a scoring matrix that reflects the residue preference for different positions of the peptide was generated (supplemental Table S10). The scoring matrix was subsequently imported into the computer program SMALI (36) to predict candidate binding proteins for the Numb PTB domain at the genome level. To identify high probability

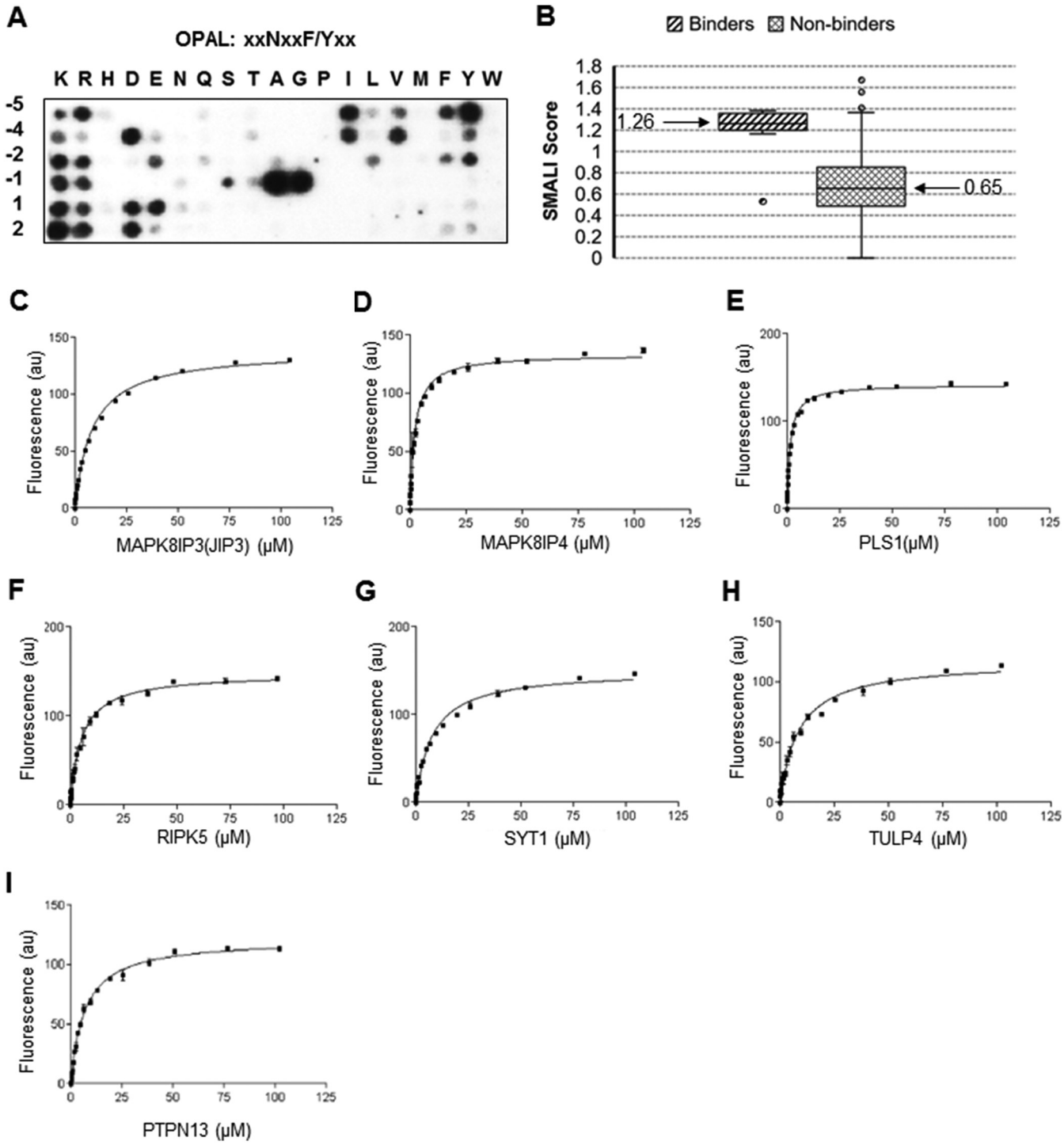

FIG. 5. **Defining Numb PTB domain specificity by OPAL.** *A*, Binding pattern of the dNumb PTB domain on an OPAL membrane with the degenerate sequence xxNxx[F/Y]xx. *B*, A box plot showing the distribution of true binders (Table I) and non-binders (from Fig. 3*A*) relative to the corresponding SMALI score. The medium value for true binders and non-binders are shown. *C–I*, Binding curves for representative peptides with a SMALI score $>$ 1.3. See Table I for peptide sequences and K_d values.

binders, we set the cut-off score in SMALI to 1.3 according to the distribution pattern of validated binders (based on the K_d value listed in Table I and supplemental Table S9) and non-binders (based on Fig. 3*A*) (Fig. 5*C*). Using this cut-off, we identified 711 human proteins from the UniProt database (37) (supplemental Table S11) that contain at least one high probability Numb PTB-binding sequence. Molecular function annotation (46) revealed that protein phosphatases, tyrosine

phosphatases, were highly enriched in the SMALI-predicted PTB interactome. Intriguingly, channel proteins and proteins involved in vesicular transport were also enriched. To evaluate the accuracy of the prediction, we selected representative examples from the predicted binding peptides (with the SMALI score >1.3) and measured their affinities for the dPTB domain by fluorescence polarization. Peptides representing binding sequences for the phosphotyrosine phosphatases PTP-13, the Ser/Thr kinase RIPK5, the JNK signaling scaffolds MAPK8IP3 (JIP3) and MAPK8IP4 (JIP4), and the membrane trafficking protein SYT1, the Tubby family transcription factor TULP4, and the actin-binding protein PLS1 exhibited high affinities for the Numb PTB domain with K_d values ranging from 1.5 to 8.5 μM (Fig. 5*C*–5*I* and Table I). These data indicate that specificity-based SMALI prediction can predict binding partners with K_d values expected for interactions mediated by a PTB domain or another modular interaction domain (47, 48).

Functional Analysis of the Numb Interactome—Both the TKs and STKs were enriched in the Numb-binding proteins identified from the Protoarray (Fig. 2*D*–2*E* and supplemental Fig. S7*A*). In contrast, protein phosphatases, especially tyrosine phosphatases, are enriched in proteins predicted to bind the Numb PTB domain by SMALI (supplemental Fig. S7*B*). If we combine data from both the ProtoArray screening and SMALI prediction, then tyrosine kinases, serine/threonine kinases and tyrosine phosphatases are the most enriched protein categories in the resulting Numb interactome (Fig. 6*A*). It is intriguing to note that the 42 TKs identified as Numb-binding proteins occupy essentially all branches of the human kinome phylogeny tree (Fig. 6*B*). Our data strongly implicates Numb in regulating the activity and/or function of tyrosine kinases via direct binding to these proteins through its PTB domain.

DISCUSSION

Mapping the PPI network in a systematic manner is key to decoding the human proteome and deciphering the function of individual proteins. In this regard, several high-throughput approaches have been developed in the past decades for PPI mapping at a large scale. These include mass spectrometry (MS) based approaches such as TAP (tandem affinity purification) and BioID, luminescence-based interactome mapping, and yeast two-hybrid (Y2H) screen (32, 33, 49). A limitation of these approaches is that they cannot provide information about the binding sites in most cases. To complement these approaches, protein and peptide array-based assays have been developed for systematic PPI identification *in vitro*. For example, peptide and protein arrays have been used to identify PPI networks mediated by the Src homology 2 (SH2) and 3 (SH3) domains (50, 51). Recently, we have developed a bidirectional protein-peptide array screening method to map the PPI network mediated by the SH2 domains and immunoreceptor-tyrosine based regulatory motifs (52).

In this study, we developed an integrated approach combining protein microarray, peptide spot array, OPAL screening and bioinformatics analysis to identify binding partners for modular interaction domains and applied this approach to deciphering the Numb PTB domain interactome. We focused on Numb because of its broad functions in animal development and disease pathogenesis (53). The IntAct (54) database lists 30 Numb-interacting proteins (supplemental Table S12). Although some of these interactions are direct and may involve the PTB domain, others may be indirect or involve other regions of Numb. Furthermore, the Numb PTB domain could bind a partner through peptide motifs that are either non-phosphorylated or phosphorylated (such Nxx[Y/F] (39) and GPpY (43)) or through domain-domain interactions (55). It is also highly likely that additional modes of ligand binding exist for the Numb PTB domain. The multiple modes of ligand binding by the Numb PTB domain provides a rationale for the generally low re-identification rate of known binding partners from either the ProtoArray screening or SMALI prediction. Of the 11 known binding partners of Numb that were included in the Protoarray, four were identified in our screen (supplemental Table S12). The 7 Numb-binding proteins that were missed in our protein array screen may not bind directly to Numb or its PTB domain. The SMALI prediction captured four known Numb-binding proteins (supplemental Table S12), reflecting again that many Numb-protein interactions do not necessarily involve the PTB domain or are mediated by the Nxx[Y/F] motif.

Nevertheless, combining ProtoArray screening and specificity-based prediction, we identified an unprecedented ~900 proteins that could potentially interact with Numb. That the Numb PTB domain is capable of putatively binding to such a large number of proteins is mind-boggling. Although stringent cut-off values (*i.e.* Z-score >2 or SMALI score >1.3) were applied in the identification of binding partners, it is inevitable that false positives have been included in the resulting interactome. The use of the dNumb PTB domain as the probe for array screening might have contributed to false positives. The dNumb PTB domain is more stable than its mammalian counterparts (38, 39) and appears to bind more strongly than the latter to the full-length proteins tested (Fig. 3). On the other hand, the large number of binding partners may reflect the promiscuity of the PTB domain, and likely, modular domains in general. Along this line, the human genome encodes only a few dozens of PTB domains (20), yet thousands of proteins containing the Nxx[Y/F] motif. Therefore a given PTB domain has the potential to interact with hundreds or even more proteins containing the motif. Similarly, the identified phosphotyrosine sites far outnumber the SH2 domains encoded by the human genome, and PxxP motif-containing proteins far outnumber the SH3 domains. Therefore, it is likely that these modular domains might sample through multiple potential binding partners in the cell before a productive interaction could occur. Notwithstanding the intrinsic promiscuity of the modular domains, the specificity of modular domain-medi-

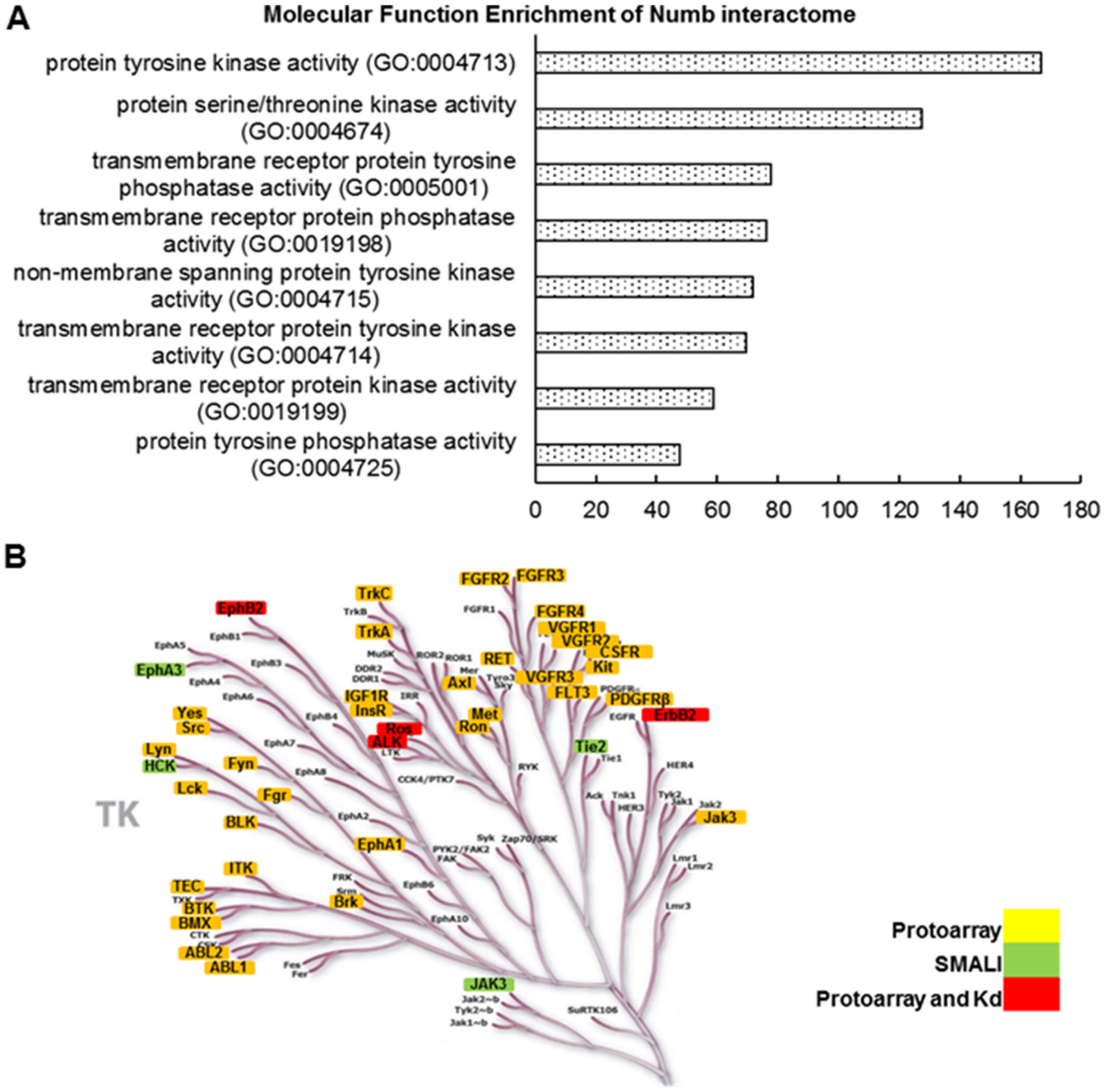

FIG. 6. **The Numb interactome is enriched for proteins involved in phosphorylation signaling.** *A*, Molecular function enrichment for the Numb-binding proteins identified in this study. *B*, Distribution of Numb-binding TKs in the human kinome phylogeny tree. Fig. reproduced courtesy of Cell Signaling Technology, Inc.

ated protein-protein interactions in the cell may be regulated by protein expression, modification, and subcellular localization, by additional regions in the interacting pairs or by other proteins that may function as scaffolds (47).

Although further investigations are warranted to define the physiological relevance of the vast number of interactions identified in the present study, it is tempting to speculate the functions of Numb based on the expansive network of putative binding partners. Of the proteins identified from both the ProtoArray screening and SMALI prediction, protein kinases and phosphatases, especially tyrosine kinases and phosphotyrosine phosphatases, are most abundantly represented (Fig. 6*A*). It is rather intriguing that ~50% of all TKs are capable of binding to the Numb PTB domain (Fig. 6*B*), some of which contain high affinity binding motifs and/or are confirmed for binding in cells (Fig. 3). This suggests that Numb may play a

general role in regulating protein phosphorylation and kinase signaling through direct interactions with multiple kinases and phosphatases. Prior to this study, Numb has been shown to interact with three RTKs, namely EphB2, TrkB and EGFR. The Numb-EphB2 interaction plays a role in ephrin-B1-induced spine development and maturation (56). The Numb-TrkB interaction alters TrkB's chemotactic response to BDNF (brain-derived neurotrophic factor) ligand (17). It has been shown that Numb binding decreases EGFR protein level to regulate the fate of glioblastoma stem-like cells (57). However, little direct evidence has been provided in these studies to make the conclusion that Numb directly interact with these RTKs. Here, we show that RTKs are highly enriched in the Numb interactome; and oncogenic RTKs such as ALK and ErbB2 can directly interact with Numb in the cell. Given the established function of Numb in endocytosis, it is likely that Numb may regulate the endocytosis or trafficking of these RTKs and other membrane proteins. In this regard, Numb may play a role as a critical regulator of trans-membrane signal transduction by altering membrane receptor abundance, particularly in the context of growth factor stimulated RTK signaling. Further experiments are also needed to investigate if Numb is involved in the endocytosis or intracellular trafficking of PTPs, thereby adding an extra layer of regulation to phosphotyrosine signaling dynamics.

Besides TK and PTPs, transcription factors such as TULP4 have also been identified in the putative Numb interactome. We reported previously that Numb binds to the transcriptional factor p53 through its PTB domain and the Numb-p53 interaction regulates p53 stability and the transcription of several genes involved in DNA damage response or apoptosis (58). Nevertheless, very few nuclear binding partners have been identified for Numb to date, even though Numb can localize to the nucleus (29, 40, 59). It is also not fully understood how Numb alters transcription activity at a molecular level. Given the potential for Numb to interact with a wide array of different proteins, it is possible that Numb may regulate gene transcription by directly binding to transcriptional factors.

In conclusion, we have identified the largest putative Numb interactome reported to date, revealing a general role for Numb in protein kinase signaling. Because of the pivotal role of protein kinases in tumorigenesis, our work suggests that Numb is a potential therapeutic target for cancers driven by aberrant kinase activation. Future studies focusing on elucidating the physiological relevance of the putative Numb interactome will undoubtedly shed new light on how Numb regulates different cellular processes under normal or pathological conditions.

Acknowledgments—We thank Wen Qin for critical reading of the manuscript.

* This work was supported in part by grants (to SSL) from the Canadian Institute of Health Research (CIHR) and the Canadian Cancer Society Research Institute. SSL held a Canada Research Chair in Functional Genomics and Cellular Proteomics.

S This article contains supplemental Figures and Tables.

‡‡ To whom correspondence should be addressed: Department of Biochemistry and the Siebens-Drake Medical Research Institute, Schulich School of Medicine and Dentistry, Western University, London, Ontario N6A 5C1, Canada. E-mail: sli@uwo.ca.

Author contributions: R.W., X.L., and C.V. performed research; R.W., T.K., H.L., L.L., E.L., and N.H. analyzed data; R.W. and S.S.-C.L. wrote the paper; S.S.-C.L. designed the research.

REFERENCES

1. Arkin, M. R., and Wells, J. A. (2004) Small-molecule inhibitors of protein-protein interactions: progressing towards the dream. *Nat. Rev. Drug Discov.* **3,** 301–317
2. Uemura, T., Shepherd, S., Ackerman, L., Jan, L. Y., and Jan, Y. N. (1989) numb, a gene required in determination of cell fate during sensory organ formation in Drosophila embryos. *Cell* **58,** 349–360
3. Rhyu, M. S., Jan, L. Y., and Jan, Y. N. (1994) Asymmetric distribution of numb protein during division of the sensory organ precursor cell confers distinct fates to daughter cells. *Cell* **76,** 477–491
4. Zhong, W., Jiang, M. M., Schonemann, M. D., Meneses, J. J., Pedersen, R. A., Jan, L. Y., and Jan, Y. N. (2000) Mouse numb is an essential gene involved in cortical neurogenesis. *Proc. Natl. Acad. Sci. U.S.A.* **97**, 6844–6849
5. Gulino, A., Di Marcotullio, L., and Screpanti, I. (2010) The multiple functions of Numb. *Exp. Cell Res.* **316,** 900–906
6. Juven-Gershon, T., Shifman, O., Unger, T., Elkeles, A., Haupt, Y., and Oren, M. (1998) The Mdm2 oncoprotein interacts with the cell fate regulator Numb. *Mol. Cell. Biol.* **18,** 3974
7. Nie, J., McGill, M. A., Dermer, M., Dho, S. E., Wolting, C. D., and McGlade, C. J. (2002) LNX functions as a RING type E3 ubiquitin ligase that targets the cell fate determinant Numb for ubiquitin-dependent degradation. *EMBO J.* **21**, 93–102
8. Di Marcotullio, L., Ferretti, E., Greco, A., De Smaele, E., Po, A., Sico, M. A., Alimandi, M., Giannini, G., Maroder, M., Screpanti, I., and Gulino, A. (2006) Numb is a suppressor of Hedgehog signalling and targets Gli1 for Itch-dependent ubiquitination. *Nat. Cell Biol.* **8,** 1415–1423
9. Susini, L., Passer, B. J., Amzallag-Elbaz, N., Juven-Gershon, T., Prieur, S., Privat, N., Tuynder, M., Gendron, M. C., Israel, A., Amson, R., Oren, M., and Telerman, A. (2001) Siah-1 binds and regulates the function of Numb. *Proc. Natl. Acad. Sci. U.S.A.* **98,** 15067–15072
10. Salcini, A. E., Confalonieri, S., Doria, M., Santolini, E., Tassi, E., Minenkova, O., Cesareni, G., Pelicci, P. G., and Di Fiore, P. P. (1997) Binding specificity and in vivo targets of the EH domain, a novel protein-protein interaction module. *Genes Dev.* **11,** 2239–2249
11. Berdnik, D., Torok, T., Gonzalez-Gaitan, M., and Knoblich, J. A. (2002) The endocytic protein alpha-Adaptin is required for numb-mediated asymmetric cell division in Drosophila. *Developmental Cell* **3,** 221–231
12. Dho, S. E., French, M. B., Woods, S. A., and McGlade, C. J. (1999) Characterization of four mammalian numb protein isoforms. Identification of cytoplasmic and membrane-associated variants of the phosphotyrosine binding domain. *J. Biol. Chem.* **274,** 33097–33104
13. McGill, M. A., Dho, S. E., Weinmaster, G., and McGlade, C. J. (2009) Numb regulates post-endocytic trafficking and degradation of Notch1. *J. Biol. Chem.* **284,** 26427–26438
14. Nishimura, T., and Kaibuchi, K. (2007) Numb controls integrin endocytosis for directional cell migration with aPKC and PAR-3. *Developmental Cell* **13,** 15–28
15. Wang, Z., Sandiford, S., Wu, C., and Li, S. S. (2009) Numb regulates cell-cell adhesion and polarity in response to tyrosine kinase signaling. *EMBO J.* **28**, 2360–2373
16. Sato, K., Watanabe, T., Wang, S., Kakeno, M., Matsuzawa, K., Matsui, T., Yokoi, K., Murase, K., Sugiyama, I., Ozawa, M., and Kaibuchi, K. (2011) Numb controls E-cadherin endocytosis through p120 catenin with aPKC. *Mol. Biol. Cell* **22,** 3103–3119
17. Zhou, P., Alfaro, J., Chang, E. H., Zhao, X., Porcionatto, M., and Segal, R. A. (2011) Numb links extracellular cues to intracellular polarity machinery to promote chemotaxis. *Dev Cell* **20**, 610–622
18. Letunic, I., Doerks, T., and Bork, P. (2015) SMART: recent updates, new developments and status in 2015. *Nucleic Acids Res.* **43,** D257–D260

19. Schultz, J., Milpetz, F., Bork, P., and Ponting, C. P. (1998) SMART, a simple modular architecture research tool: identification of signaling domains. *Proc. Natl. Acad. Sci. U.S.A.* **95,** 5857–5864
20. Uhlik, M. T., Temple, B., Bencharit, S., Kimple, A. J., Siderovski, D. P., and Johnson, G. L. (2005) Structural and evolutionary division of phosphotyrosine binding (PTB) domains. *J. Mol. Biol.* **345**, 1–20
21. Kinoshita, A., Whelan, C. M., Smith, C. J., Mikhailenko, I., Rebeck, G. W., Strickland, D. K., and Hyman, B. T. (2001) Demonstration by fluorescence resonance energy transfer of two sites of interaction between the low-density lipoprotein receptor-related protein and the amyloid precursor protein: Role of the intracellular adapter protein Fe65. *J. Neurosci.* **21,** 8354–8361
22. Howell, B. W., Lanier, L. M., Frank, R., Gertler, F. B., and Cooper, J. A. (1999) The disabled 1 phosphotyrosine-binding domain binds to the internalization signals of transmembrane glycoproteins and to phospholipids. *Mol. Cell. Biol.* **19,** 5179–5188
23. Guenette, S. Y., Chen, J., Ferland, A., Haass, C., Capell, A., and Tanzi, R. E. (1999) hFE65L influences amyloid precursor protein maturation and secretion. *J. Neurochem.* **73,** 985–993
24. Hill, K., Li, Y., Bennett, M., McKay, M., Zhu, X., Shern, J., Torre, E., Lah, J. J., Levey, A. I., and Kahn, R. A. (2003) Munc18 interacting proteins: ADP-ribosylation factor-dependent coat proteins that regulate the traffic of beta-Alzheimer's precursor protein. *J. Biol. Chem.* **278,** 36032–36040
25. Chien, C. T., Wang, S., Rothenberg, M., Jan, L. Y., and Jan, Y. N. (1998) Numb-associated kinase interacts with the phosphotyrosine binding domain of Numb and antagonizes the function of Numb in vivo. *Mol. Cell. Biol.* **18,** 598–607
26. Chang, D. D., Wong, C., Smith, H., and Liu, J. (1997) ICAP-1, a novel beta1 integrin cytoplasmic domain-associated protein, binds to a conserved and functionally important NPXY sequence motif of beta1 integrin. *J. Cell Biol.* **138,** 1149–1157
27. Filardo, E. J., Brooks, P. C., Deming, S. L., Damsky, C., and Cheresh, D. A. (1995) Requirement of the NPXY motif in the integrin beta 3 subunit cytoplasmic tail for melanoma cell migration in vitro and in vivo. *J. Cell Biol.* **130,** 441–450
28. Guo, M., Jan, L. Y., and Jan, Y. N. (1996) Control of daughter cell fates during asymmetric division: interaction of Numb and Notch. *Neuron* **17,** 27–41
29. Dhami, G. K., Liu, H., Galka, M., Voss, C., Wei, R., Muranko, K., Kaneko, T., Cregan, S. P., Li, L., and Li, S. S. (2013) Dynamic methylation of Numb by Set8 regulates its binding to p53 and apoptosis. *Mol. Cell* **50,** 565–576
30. McGill, M. A., and McGlade, C. J. (2003) Mammalian numb proteins promote Notch1 receptor ubiquitination and degradation of the Notch1 intracellular domain. *J. Biol. Chem.* **278,** 23196–23203
31. Colaluca, I. N., Tosoni, D., Nuciforo, P., Senic-Matuglia, F., Galimberti, V., Viale, G., Pece, S., and Di Fiore, P. P. (2008) NUMB controls p53 tumour suppressor activity. *Nature* **451,** 76–80
32. Lamesch, P., Li, N., Milstein, S., Fan, C., Hao, T., Szabo, G., Hu, Z., Venkatesan, K., Bethel, G., Martin, P., Rogers, J., Lawlor, S., McLaren, S., Dricot, A., Borick, H., Cusick, M. E., Vandenhaute, J., Dunham, I., Hill, D. E., and Vidal, M. (2007) hORFeome v3.1: A resource of human open reading frames representing over 10,000 human genes. *Genomics* **89,** 307–315
33. Blasche, S., and Koegl, M. (2013) Analysis of protein-protein interactions using LUMIER assays. *Methods Mol. Biol.* **1064,** 17–27
34. Qin, H., Percival-Smith, A., Li, C., Jia, C. Y., Gloor, G., and Li, S. S. (2004) A novel transmembrane protein recruits numb to the plasma membrane during asymmetric cell division. *J. Biol. Chem.* **279,** 11304–11312
35. Huang, H., Li, L., Wu, C., Schibli, D., Colwill, K., Ma, S., Li, C., Roy, P., Ho, K., Songyang, Z., Pawson, T., Gao, Y., and Li, S. S. (2008) Defining the specificity space of the human SRC homology 2 domain. *Mol. Cell. Proteomics* **7,** 768–784
36. Li, L., Wu, C., Huang, H., Zhang, K., Gan, J., and Li, S. S. (2008) Prediction of phosphotyrosine signaling networks using a scoring matrix-assisted ligand identification approach. *Nucleic Acids Res.* **36,** 3263–3273
37. The UniProt, C. (2017) UniProt: the universal protein knowledgebase. *Nucleic Acids Res.* **45,** D158–D169
38. Li, S. C., Zwahlen, C., Vincent, S. J. F., Jane McGlade, C., Kay, L. E., Pawson, T., and Forman-Kay, J. D. (1998) Structure of a Numb PTB domain-peptide complex suggests a basis for diverse binding specificity. *Nat. Structural Biol.* **5,** 1075–1083
39. Zwahlen, C., Li, S. C., Kay, L. E., Pawson, T., and Forman-Kay, J. D. (2000) Multiple modes of peptide recognition by the PTB domain of the cell fate determinant Numb. *EMBO J.* **19,** 1505–1515
40. Martin-Blanco, N. M., Checquolo, S., Del Gaudio, F., Palermo, R., Franciosa, G., Di Marcotullio, L., Gulino, A., Canelles, M., and Screpanti, I. (2014) Numb-dependent integration of pre-TCR and p53 function in T-cell precursor development. *Cell Death Dis.* **5,** e1472
41. Smith, C. A., Lau, K. M., Rahmani, Z., Dho, S. E., Brothers, G., She, Y. M., Berry, D. M., Bonneil, E., Thibault, P., Schweisguth, F., Le Borgne, R., and McGlade, C. J. (2007) aPKC-mediated phosphorylation regulates asymmetric membrane localization of the cell fate determinant Numb. *EMBO J.* **26,** 468–480
42. Tokumitsu, H., Hatano, N., Inuzuka, H., Sueyoshi, Y., Yokokura, S., Ichimura, T., Nozaki, N., and Kobayashi, R. (2005) Phosphorylation of Numb family proteins. Possible involvement of Ca2+/calmodulin-dependent protein kinases. *J. Biol. Chem.* **280,** 35108–35118
43. Li, S. C., Songyang, Z., Vincent, S. J., Zwahlen, C., Wiley, S., Cantley, L., Kay, L. E., Forman-Kay, J., and Pawson, T. (1997) High-affinity binding of the Drosophila Numb phosphotyrosine-binding domain to peptides containing a Gly-Pro-(p)Tyr motif. *Proc. Natl. Acad. Sci. U.S.A.* **94,** 7204–7209
44. Li, S. C., Lai, K. M., Gish, G. D., Parris, W. E., van der Geer, P., Forman-Kay, J., and Pawson, T. (1996) Characterization of the phosphotyrosine-binding domain of the Drosophila Shc protein. *J. Biol. Chem.* **271,** 31855–31862
45. Wilhelm, M., Schlegl, J., Hahne, H., Gholami, A. M., Lieberenz, M., Savitski, M. M., Ziegler, E., Butzmann, L., Gessulat, S., Marx, H., Mathieson, T., Lemeer, S., Schnatbaum, K., Reimer, U., Wenschuh, H., Mollenhauer, M., Slotta-Huspenina, J., Boese, J. H., Bantscheff, M., Gerstmair, A., Faerber, F., and Kuster, B. (2014) Mass-spectrometry-based draft of the human proteome. *Nature* **509,** 582–587
46. Kuleshov, M. V., Jones, M. R., Rouillard, A. D., Fernandez, N. F., Duan, Q., Wang, Z., Koplev, S., Jenkins, S. L., Jagodnik, K. M., Lachmann, A., McDermott, M. G., Monteiro, C. D., Gundersen, G. W., and Ma'ayan, A. (2016) Enrichr: a comprehensive gene set enrichment analysis web server 2016 update. *Nucleic Acids Res.* **44,** W90–W97
47. Li SS. (2005) Specificity and versatility of SH3 and other proline-recognition domains: structural basis and implications for cellular signal transduction. *Biochem. J.* **390,** 641–653
48. Kaneko, T., Li, L., and Li, S. S. (2008) The SH3 domain–a family of versatile peptide- and protein-recognition module. *Frontiers Biosci.* **13,** 4938–4952
49. Roux, K. J., Kim, D. I., and Burke, B. (2013) BioID: a screen for protein-protein interactions. *Current Protocols Protein Sci.* **74**, Unit 19 23
50. Wu, C., Ma, M. H., Brown, K. R., Geisler, M., Li, L., Tzeng, E., Jia, C. Y., Jurisica, I., and Li, S. S. (2007) Systematic identification of SH3 domain-mediated human protein-protein interactions by peptide array target screening. *Proteomics* **7,** 1775–1785
51. Tinti, M., Kiemer, L., Costa, S., Miller, M. L., Sacco, F., Olsen, J. V., Carducci, M., Paoluzi, S., Langone, F., Workman, C. T., Blom, N., Machida, K., Thompson, C. M., Schutkowski, M., Brunak, S., Mann, M., Mayer, B. J., Castagnoli, L., and Cesareni, G. (2013) The SH2 domain interaction landscape. *Cell Reports* **3,** 1293–1305
52. Liu, H., Li, L., Voss, C., Wang, F., Liu, J., and Li, S. S. (2015) A Comprehensive Immunoreceptor Phosphotyrosine-based Signaling Network Revealed by Reciprocal Protein-Peptide Array Screening. *Mol. Cell. Proteomics* **14**, 1846–1858
53. Pece, S., Confalonieri, S., P., R. R., Di Fiore, P. P. (2011) NUMB-ing down cancer by more than just a NOTCH. *Biochim. Biophys. Acta* **1815**, 26–43
54. Orchard, S., Ammari, M., Aranda, B., Breuza, L., Briganti, L., Broackes-Carter, F., Campbell, N. H., Chavali, G., Chen, C., del-Toro, N., Duesbury, M., Dumousseau, M., Galeota, E., Hinz, U., Iannuccelli, M., Jagannathan, S., Jimenez, R., Khadake, J., Lagreid, A., Licata, L., Lovering, R. C., Meldal, B., Melidoni, A. N., Milagros, M., Peluso, D., Perfetto, L., Porras, P., Raghunath, A., Ricard-Blum, S., Roechert, B., Stutz, A., Tognolli, M., van Roey, K., Cesareni, G., and Hermjakob, H. (2014) The MIntAct project-IntAct as a common curation platform for 11 molecular interaction databases. *Nucleic Acids Res.* **42,** D358–D363

55. Nie, J., Li, S. S., and McGlade, C. J. (2004) A novel PTB-PDZ domain interaction mediates isoform-specific ubiquitylation of mammalian Numb. *J. Biol. Chem.* **279,** 20807–20815
56. Nishimura, T., Yamaguchi, T., Tokunaga, A., Hara, A., Hamaguchi, T., Kato, K., Iwamatsu, A., Okano, H., and Kaibuchi, K. (2006) Role of numb in dendritic spine development with a Cdc42 GEF intersectin and EphB2. *Mol. Biol. Cell* **17,** 1273–1285
57. Jiang, X., Xing, H., Kim, T. M., Jung, Y., Huang, W., Yang, H. W., Song, S., Park, P. J., Carroll, R. S., and Johnson, M. D. (2012) Numb regulates glioma stem cell fate and growth by altering epidermal growth factor receptor and Skp1-Cullin-F-box ubiquitin ligase activity. *Stem Cells* **30**, 1313–1326
58. Bechara, E. G., Sebestyen, E., Bernardis, I., Eyras, E., and Valcarcel, J. (2013) RBM5, 6, and 10 differentially regulate NUMB alternative splicing to control cancer cell proliferation. *Mol. Cell* **52,** 720–733
59. Wang, C., Cui, T., Feng, W., Li, H., and Hu, L. (2015) Role of Numb expression and nuclear translocation in endometrial cancer. *Oncol. Lett.* **9,** 1531–1536